Phenotypic Mixing between Different Hepadnavirus Nucleocapsid Proteins Reveals C Protein Dimerization To Be *cis* Preferential

CHRISTOPHER CHANG,[1,3] SILIANG ZHOU,[2] DON GANEM,[3]* AND DAVID N. STANDRING[1,2]*

Department of Biochemistry and Biophysics,[1] Hormone Research Institute,[2] and Departments of Microbiology and Medicine and Howard Hughes Medical Institute,[3] University of California Medical Center, San Francisco, California 94143

Hepadnaviruses encode a single core (C) protein which assembles into a nucleocapsid containing the polymerase (P) protein and pregenomic RNA during viral replication in hepatocytes. We examined the ability of heterologous hepadnavirus C proteins to cross-oligomerize. Using a two-hybrid assay in HepG2 cells, we observed cross-oligomerization among the core proteins from hepatitis B virus (HBV), woodchuck hepatitis virus, and ground squirrel hepatitis virus. When expressed in *Xenopus* oocytes, in which hepadnavirus C proteins form capsids, the C polypeptides from woodchuck hepatitis virus and ground squirrel hepatitis virus, but not duck hepatitis B virus, can efficiently coassemble with an epitope-tagged HBV core polypeptide to form mixed capsids. However, when two different core mRNAs are coexpressed in oocytes the core monomers show a strong preference for forming homodimers rather than heterodimers. This holds true even for coexpression of two HBV C proteins differing only by an epitope tag, suggesting that core monomers are not free to diffuse and associate with other monomers. Thus, mixed capsids result from aggregation of different species of homodimers.

The core (C) protein of hepatitis B virus (HBV) plays a major role in viral morphogenesis. Core polypeptides, the polymerase (P), and the pregenomic RNA assemble to form the nucleocapsid during viral replication in hepatocytes. The nucleocapsid, in turn, interacts with internal cellular membranes that contain HBV envelope glycoproteins to produce enveloped virions. Several laboratories have demonstrated that core protein expressed in the absence of all other viral products can spontaneously assemble into capsid particles in hosts as divergent as bacteria (3, 6), the yeast *Saccharomyces cerevisiae* (13), insect cells (2), or *Xenopus* oocytes (21). Nevertheless, the pathway for capsid assembly remains incompletely understood. Zhou and Standring (20, 21) have shown that in the *Xenopus* oocyte system, unassembled core protein exists in a dimer pool that serves as a precursor to capsids. Electron microscopy and velocity sedimentation studies have failed to detect in vivo higher-order multimer intermediates often seen in the assembly of other animal virus capsids (20).

Efforts to identify regions of the 185-amino-acid (aa) C protein that are critical for capsid formation have focused primarily on the arginine-rich C-terminal tail (2, 3). In various heterologous systems expressing core protein, deletions containing the N-terminal 144 aa produce stable capsids, demonstrating that the Arg-rich tail is not necessary for capsid assembly (2, 3). Moreover, assembly is tolerant of heterologous sequences placed at the N terminus, at the C terminus, and within an immunodominant loop of core protein (4, 5, 16). However, C-terminal truncations resulting in C proteins shorter than 144 residues abrogate core particle assembly.

To further characterize C-C interactions involved in capsid assembly, we examined the ability of mammalian and avian hepadnavirus C proteins to interact with each other. We used both expression in *Xenopus* oocytes and a mammalian cell-based two-hybrid system. The two-hybrid strategy originally developed by Fields and Song (9) to detect protein-protein interactions relies on the modular nature of the yeast GAL4 DNA-binding and transactivation domains. Fearon and colleagues modified this system to study interactions in mammalian cells by using the herpes simplex virus VP16 transactivation domain (8). Luban et al. have applied this strategy to detect multimerization of Gag polyprotein from both human immunodeficiency virus (HIV) and Moloney murine leukemia virus (MuLV) (11).

In this communication, we report that HBV core proteins (HBV-C) fused to GAL4 and VP16 domains interact in the two-hybrid assay and that this interaction behaves as predicted from in vivo studies of capsid formation. Using this two-hybrid assay, we demonstrate cross-oligomerization among the core proteins from HBV, woodchuck hepatitis virus (WHV), and ground squirrel hepatitis virus (GSHV). Consistent with this finding, when expressed in *Xenopus* oocytes, the C proteins from WHV and GSHV, but not duck hepatitis B virus (DHBV), efficiently coassemble with HBV C protein to form mixed capsids. Surprisingly, however, when two different C protein mRNAs are translated in the oocyte, the C polypeptides show a marked preference for forming homodimers rather than heterodimers; thus, mixed capsids are aggregates of different species of homodimers.

MATERIALS AND METHODS

Materials. Restriction enzymes were purchased from New England Biolabs and used as specified by the manufacturer. Radionucleotides were purchased from Amersham Corp. or New England Nuclear. Monoclonal antibody (MAb) 18/7, the MAb directed against the L epitope, was kindly provided by Volker Bruss and Wolfram Gerlich. The rabbit polyclonal anti-HBV-C-antibody was purchased from Dako Corp. Anti-DHBV-C was kindly provided by Jesse Summers.

Plasmids and RNAs. All HBV nucleotide positions are numbered from the unique *Eco*RI site of HBV subtype adw2. Core fusion proteins with GAL4 or VP16 were made by subcloning appropriate restriction or PCR-amplified frag-

---

* Corresponding authors.

ments into the expression vectors pGAL0 and pNLVP16, which, along with the reporter plasmid pG5E1bCAT, were described earlier (8) and kindly provided by Eric Fearon. In brief, pGAL0 encodes the DNA-binding domain of GAL4, extending from aa 1 to 147, followed by polylinker sequence. pNLVP16 contains aa 411 to 455 of the HSV VP16 transactivation domain followed by polylinker sequence. Full-length HBV, WHV, and GSHV core fusions were made by subcloning a 581-bp StyI fragment into the polylinker of pGAL0 and pNLVP16 to create an in-frame fusion with the C terminus of the GAL4 or VP16 domain. C-terminal truncations HBc1-144 and HBc1-117 were engineered by deleting sequence from BspEI and SspI, respectively, to the polylinker; HBc29-168 was constructed by inserting a 445-bp BglII fragment into the pGAL4 polylinker; HBc38-183 was constructed by inserting a 449-bp TaqI-StyI fragment into the pNLVP16 polylinker.

To create SP6 expression vectors, the fragments spanning the core open reading frames of WHV, GSHV, and DHBV were generated by PCR amplification so as to include an NcoI site at the 5' end and a BstEII site at the 3' end. These fragments were cloned into the NcoI and BstEII sites of a derivative of pSP64T. This strategy puts the core sequences between the translation-enhancing 5' and 3' untranslated region sequences of the β-globin gene. Plasmids pSP64T-C and Δ157 are described in detail elsewhere (19). Briefly, pSP64T-C contains the 581-bp StyI fragment from HBV adw2 (nucleotides 1880 to 2461) cloned into the BglII site of pSP64T. Δ157 encodes a core deletion containing the first 157 aa fused in frame to the last two residues of core protein. The L epitope tag has been previously described (14b). We modified the original L epitope sequence with a silent base change that would introduce a BamHI site: 5'GATCATCAGTTGGATC CTGCATTCGGAGCCAACTCA 3'. The L epitope in Δ157L and HBV-CL is bordered by core residues 78 and 80, deleting residue 79, in the immunodominant loop of core. It was introduced into this site by ligation at the BamHI site of the two PCR-amplified halves of the core open reading frame flanking the L epitope. SP6 expression constructs were verified by sequence analysis.

In vitro transcription. Synthetic transcripts were prepared by using SP6 polymerase (Promega). Transcription reaction mixtures were treated with DNase, phenol extracted, ethanol precipitated, resuspended into H_2O, and stored at $-70°C$ until required for microinjection.

Transfections. HepG2 cells were grown on 100-mm-diameter dishes in DMEH-16 medium supplemented with 10% fetal bovine serum (Gibco), 0.14% sodium bicarbonate, and 2 mM glutamine. HepG2 cells were transfected with 5 μg of each of the GAL4 and VP16 fusion constructs and the chloramphenicol acetyltransferase (CAT) reporter plasmid by the calcium phosphate coprecipitation procedure as described previously (10).

CAT activity assays. Cell extracts for CAT activity were prepared by freeze-thaw lysis of cells 48 h posttransfection. CAT activity was determined in extracts by a phase separation procedure. In brief, 5 μl of cell extract was incubated in a 100-μl volume containing 250 mM Tris-HCl (pH 8.0), 0.5 mM n-butyryl coenzyme A (Sigma), and 0.2 μCi of [14C]chloramphenicol (58.1 mCi/mmol) for 15 to 60 min at 37°C. Phase extraction was performed with an equal volume of 2:1 hexane-xylene mix, and levels of n-butyrylated chloramphenicol were determined by liquid scintillation counting. CAT activity is reported as fold increase relative to CAT activity resulting from transfection of the reporter CAT plasmid alone.

Oocyte handling and microinjection. Oocytes were cultured at 17°C in modified Barth's medium containing antibiotics

(MBSH) by standard procedures (21). Batches of 10 to 20 oocytes per experiment were injected as described previously (18) by using a programmable microinjection device (Sutter Instruments, Novato, Calif.) to control delivery of RNA (40 nl per oocyte). For experiments involving analysis of assembled capsids, metabolic labeling was initiated within 1 h of injection by placing the oocytes in MBSH containing 0.5 to 1.0 mCi of [35S]methionine and [35S]cysteine (Expresslabel; NEN) per ml and incubating them for a further 35 to 40 h at 17°C. For analysis of the intermediates in capsid assembly, the oocytes were labeled 24 h after injection for approximately 20 h. Lysates were prepared by homogenizing the oocytes in buffer (≈20 μl per oocyte) containing 50 mM Tris-HCl (pH 7.5), 1% Nonidet P-40, 100 mM NaCl, and 10 mM EDTA. Lysates were then clarified (Eppendorf centrifuge, 15,000 × g, 10 min) before fractionation.

Sucrose gradient fractionation. Oocyte lysates were layered onto either 10 to 60% (wt/vol) or 3 to 25% sucrose gradients (20, 21). For 10 to 60% gradients, 200 μl of lysate was layered onto step gradients (1.4 ml, final volume) with six 200-μl steps of 10, 20, 30, 40, 50, and 60% sucrose in 50 mM Tris-HCl (pH 7.5)–100 mM NaCl–1 mM EDTA (TNE) and centrifuged for 40 min at 4°C and 55,000 rpm in a TLS-55 swinging-bucket rotor on a TL-100 ultracentrifuge. Gradients of 3 to 25% sucrose were formed by layering 200-μl steps of 3, 5, 10, 15, 20, and 25% sucrose in TNE, immediately loaded with 200 μl of lysate, and spun at 55,000 rpm for 4 h as described above. For both sucrose gradients, 14 100-μl fractions were collected from the top of the gradient and analyzed by immunoprecipitation and sodium dodecyl sulfate (SDS)-polyacrylamide gel electrophoresis (PAGE).

Immunoprecipitations and SDS-PAGE. 35S-labeled core proteins were immunoprecipitated from ≈30 μl of each gradient fraction under native conditions, i.e., without SDS or boiling, with either a polyclonal anticore antibody (Dako) or the anti-L MAb 18/7 (15). Immune complexes were collected with Zysorbin (Zymed); after washing, the pellet was resuspended in sample buffer, and core protein was released by boiling for 10 min and analyzed on 13.5% polyacrylamide gels.

RESULTS

HBV core protein oligomerization. In order to use the two-hybrid system to characterize heterologous C-C protein interactions in replication-permissive HepG2 cells, we first demonstrated that we could detect homo-oligomerization of full-length HBV C polypeptides in this system and that the system faithfully reproduces the known aspects of C-C oligomerization.

HepG2 cells were cotransfected with plasmids expressing HBV C protein fused to the GAL4 DNA-binding domain (GAL-core) and to the VP16 transactivation domain (VP16-core), in the presence of a CAT reporter gene bearing five GAL4 DNA-binding sites. If C-C oligomerization occurs, then the VP16 activation domain will be targeted to the DNA region 5' of CAT and will activate CAT expression. Table 1 summarizes the results of CAT assays performed following these cotransfections. When the GAL4-core fusion was coexpressed with the VP16 activation domain alone, no increase in CAT activity occurred. Similarly, the VP16-core fusion did not associate with the GAL4 DNA binding domain to boost CAT expression. These controls indicate that HBV core does not associate with either the GAL4 or VP16 domain; furthermore, core by itself has no transactivating potential, nor can it bind to and activate the test promoter when it is fused to VP16. As a positive control, we showed that the α and β subunits of the

TABLE 1. Full-length HBV core protein oligomerizes[a]

GAL4 fusion	VP16 fusion	Relative CAT activity
HBc	None	1
None	HBc	1
CapZ β25	CapZ α49	40
CapZ β25	HBc	1.5
HBc	HBc	40

[a] HepG2 cells were transfected with three plasmids: a fusion construct encoding the GAL4 DNA-binding domain and a downstream protein domain of interest; a second fusion construct encoding the VP16 transactivation domain and a downstream protein domain of interest; and a CAT reporter gene with five upstream GAL4 DNA-binding sites. The test protein domains fused to the GAL4 or VP16 domains are indicated. "None" indicates that the fusion construct encodes either the GAL4 or VP16 domain alone, without a downstream domain. CAT expression levels are reported as fold increase relative to CAT activity resulting from transfection of the CAT reporter plasmid alone. HBc, HBV core antigen; CapZ, actin-capping protein.

actin-capping protein CapZ, which are known to form an α-β dimer, associated to increase CAT activity 40-fold above background levels, as shown previously (8). When GAL4-core and VP16-core clones were coexpressed, CAT gene expression likewise increased 40-fold. This result demonstrates that HBV core polypeptides can associate efficiently in the two-hybrid assay, thus enabling VP16 to transactivate the CAT reporter. The C-C interaction was specific, as shown by a lack of CAT activation when the core fusion was coexpressed with the CapZ fusion protein.

With this assay, we then evaluated the effect of truncations at the carboxy terminus of C on its ability to associate with the full-length core. As summarized in Table 2, GAL4 fused to the first 144 aa of core and without its 41-aa arginine-rich tail was nonetheless able to complex with the full-length VP16-core fusion as efficiently as the full-length GAL4-core. However, when we engineered a 68-aa deletion from the C terminus, this truncated core fusion failed to interact with full-length VP16-core fusion to activate CAT expression. This behavior closely parallels the known behavior of similar deletions in C when assayed by capsid formation in bacteria or cultured hepatocytes (3, 14).

Unlike the case for C-terminal deletions, the effect of N-terminal deletions on C-C association has not been reported. We engineered a pair of deletions and tested their interactions with full-length core. A GAL4-core fusion lacking the first 28 residues (and the C-terminal 15 residues) failed to oligomerize with core, as did a VP16-core fusion missing the first 37 aa from core. However, these data do not prove that these N-terminal residues participate in core-core interactions (either directly or indirectly); we cannot exclude that their absence might have merely disrupted the folding or stability of the fusion proteins used in this assay.

TABLE 2. C-terminal and N-terminal deletions in HBV core protein[a]

GAL4 fusion	VP16 fusion	Relative CAT activity
HBc	HBc	22
HBc1-144	HBc	23
HBc1-117	HBc	1
HBc29-168	HBc	1
HBc	HBc38-183	1

[a] See the footnote to Table 1 for details.

TABLE 3. Interactions among mammalian HBV core proteins[a]

GAL4 fusion	VP16 fusion	Relative CAT activity
HBc	HBc	23
WHc	WHc	18
GSHc	GSHc	1
WHc	HBc	72
HBc	WHc	5
GSHc	HBc	20
HBc	GSHc	1
GSHc	WHc	5
WHc	GSHc	1

[a] See the footnote to Table 1 for details. HBc, WHc, and GSHc designate core antigens from HBV, WHC, and GSHV, respectively.

Interactions among mammalian HBV core proteins. We next used this system to determine whether core proteins from the different mammalian hepadnaviruses could display hetero-oligomerize. The mammalian C proteins display significant amino acid sequence conservation. HBV-C and WHV-C differ in 46 residues; WHV-C and GSHV-C have diverged only slightly and differ in just 11 residues (17). Failure of the different mammalian C proteins to associate would imply that amino acids critical for core-core interaction have not been conserved among the viruses, whereas hetero-oligomerization would indicate that the nonconserved residues are not essential for this process.

We constructed both GAL4 and VP16 fusion proteins with WHV or GSHV C proteins. The results of the two-hybrid assays are shown in Table 3. Like the HBV fusions, the WHV constructs homo-oligomerized and activated CAT gene expression. However, the assay failed to detect homo-oligomerization between the GSHV-C fusions. Interestingly, WHV-C fusions could hetero-oligomerize with their HBV counterparts. For the GSHV-C constructs, only the GAL4-GSHV-C fusion was able to hetero-oligomerize with both its HBV-C and WHV-C partners and activate CAT expression. This observation strongly argues that the reason for the failure to detect GSHV-C homo-oligomerization in this assay is that the VP16-GSHV core fusion is either unstable or improperly folded. All attempts to detect DHBV-C homo-oligomerization failed, again most likely because of improper folding or instability of the fusion proteins.

Assembly of an epitope-tagged HBV core protein in *Xenopus* oocytes. Our results with the two-hybrid assay indicate that hetero-oligomers can form between C proteins of different species but do not establish that such mixed oligomers can proceed to capsid formation. To do this, we coexpressed different core proteins in *Xenopus* oocytes and assayed for mixed capsids by sucrose gradient purification and immunoprecipitation. For this approach to show mixed capsids, antisera that selectively recognize at least one of the individual C proteins must be available. In preliminary experiments, however, we found that WHV-C and GSHV-C are efficiently recognized by the polyclonal anti-HBV core antibody (Fig. 1, lanes 4 to 6). Therefore, we constructed a vector expressing an epitope-tagged, truncated HBV-C to serve as the HBV partner in coexpression studies; this protein can be distinguished by both its size and its reactivity with antibodies to the tag. Δ157 is a truncated HBV-C comprising the first 157 residues fused to the last 2 residues of HBV-C and assembles into capsids as efficiently as the full-length core. The 12-aa L epitope tag is from the pre-S1 region of the HBV large surface antigen and was inserted into full-length HBV-C (to generate HBV-CL)
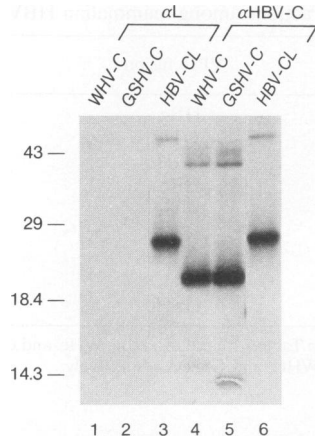
FIG. 1. Analysis of cross-reactivity with the anti-L MAb (αL) and the anti-HBV-C polyclonal antibody (αHBV-C). Lysates from ^{35}S-labeled *Xenopus* oocytes injected with the appropriate mRNA were resolved on step gradients of 10 to 60% sucrose. Fractions containing assembled capsids were combined and immunoprecipitated under nondenaturing conditions with the appropriate antibody and analyzed by SDS-PAGE on a 13.5% gel. The positions of prestained molecular mass markers are indicated in kilodaltons at the left.

and into Δ157 (generating Δ157L) between residues 78 and 80, in a predicted surface loop of the core protein that has previously been shown to be tolerant of insertions (4). To confirm that L epitope-tagged HBV C proteins could be specifically recognized by an anti-L MAb, we expressed HBV-CL (and, as controls, the wild-type C proteins of GSHV and WHV) in oocytes and examined their reactivities with the anti-L MAb 18/7 by immunoprecipitation. As shown in Fig. 1 (lanes 1 to 3), only HBV-CL was precipitable with this antibody.

To confirm that Δ157L can assemble into capsids that contain exposed L epitopes on their surface, we expressed this construct in *Xenopus* oocytes and fractionated the oocyte extracts on a step gradient of 10 to 60% sucrose; 14 fractions were collected from the gradient and analyzed by immunoprecipitation followed by SDS-PAGE, autoradiography, and PhosporImager quantitation. Similar experiments were also performed with oocytes programmed to express HBV-CL and DHBV-C. The gradient profile of Δ157L (Fig. 2B) clearly shows a capsid peak (fractions 7 to 12) that closely mirrors the profile produced by HBV-CL and DHBV-C (Fig. 2 and references 20 and 21), indicating that Δ157L indeed retains assembly competence. Immunoprecipitation under native conditions with anti-L verified that the epitope was exposed on the particle surface; core particles lacking the tag were not precipitated under these conditions (data not shown). Similar gradient profiles of WHV-C and GSHV-C (data not shown) confirm that they also assemble efficiently into capsids in *Xenopus* oocytes.

Mammalian hepadnavirus cores form mixed capsids. We next determined whether hybrid capsid particles composed of C polypeptides from different hepadnaviruses could be assembled in *Xenopus* oocytes. mRNA encoding Δ157L was coinjected into oocytes along with equal quantities of either WHV-C, GSHV-C, or DHBV-C transcripts. ^{35}S-labeled lysates were fractionated on 10 to 60% sucrose gradients into 14 fractions. Fractions 8 to 12, representing assembled capsids, were combined and immunoprecipitated with either anti-L MAb 18/7, an anti-HBV-C antibody, or an anti-DHBV-C
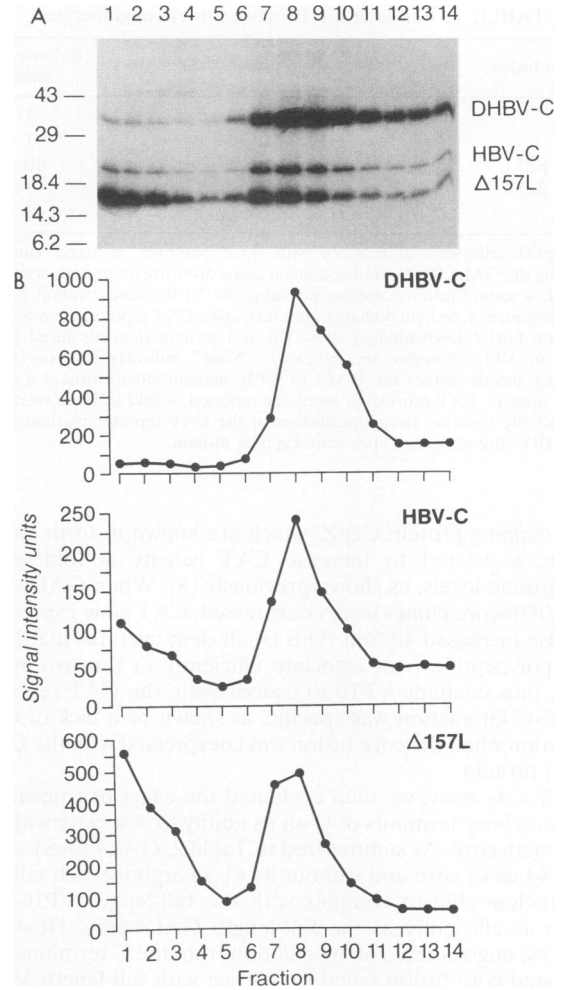

FIG. 2. Assembly of a tagged and truncated HBV core protein in *Xenopus* oocytes. (A) Lysates from ^{35}S-labeled *Xenopus* oocytes injected with mRNA encoding HBV-C, DHBV-C, or Δ157L were combined and resolved on step gradients of 10 to 60% sucrose. Fourteen fractions were collected from the top of each gradient and analyzed by immunoprecipitation under nondenaturing conditions with polyclonal anti-HBV-C and anti-DHBV-C antibodies followed by SDS-PAGE on a 13.5% gel. The gradient fractions are shown in order from the top fraction at the left (fraction 1) to the bottom fraction at the right (fraction 14). The positions of the DHBV-C, HBV-C, and Δ157L species are indicated at the right. Sizes in kilodaltons are shown at the left. (B) PhosphorImager quantitation of ^{35}S signal intensity in each fraction for the indicated core polypeptide band in the gel shown in panel A.

antibody. The labeled proteins were analyzed by SDS-PAGE (Fig. 3A). Immunoprecipitation with anti-L clearly demonstrated that Δ157L core protein forms capsids with both WHV-C and GSHV-C (lanes 1 and 4). The ratio of WHV to HBV and GSHV to HBV chains in the anti-L precipitates (lanes 1 and 4) is similar to that in the anti-HBV-C precipitates (lanes 2 and 5) and to that in the total lysate fraction (not shown). In addition, the absolute amount of WHV or GSHV core chains precipitated by anti-L is comparable to that precipitated by the broadly cross-reactive polyclonal anti-HBV-C antibodies. Together, these observations indicate that most or all of the animal hepadnavirus C polypeptides in these fractions are incorporated into mixed capsids.
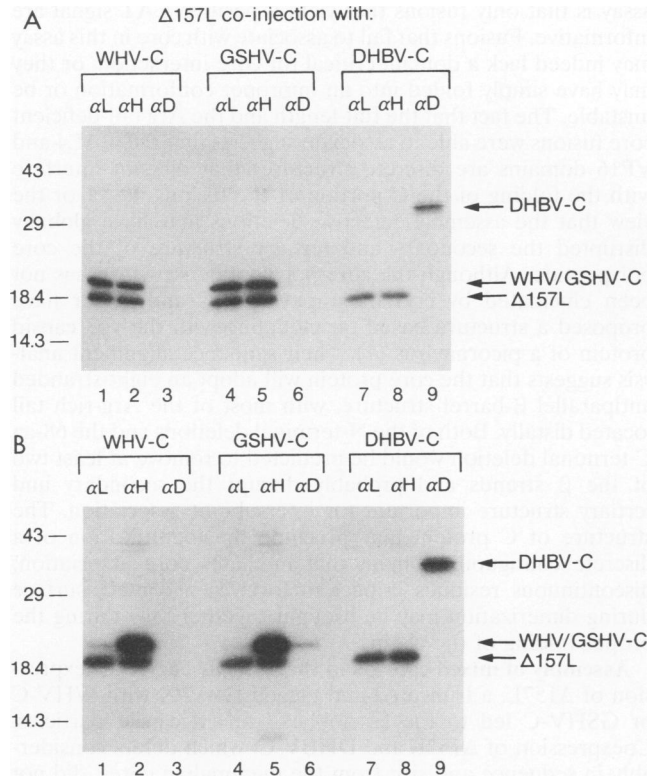
FIG. 3. Composition of capsid particles assembled in *Xenopus* oocytes coinjected with mRNAs encoding core proteins from different hepadnaviruses. (A) Oocytes were coinjected with mRNAs encoding Δ157L and either WHV-C, GSHV-C, or DHBV-C. ^{35}S-labeled lysates were resolved on step gradients of 10 to 60% sucrose. Fractions 8 to 12, containing assembled capsids, were combined and immunoprecipitated under nondenaturing conditions with either an anti-L MAb (αL) or an anti-HBV-C (αH) or anti-DHBV-C (αD) polyclonal antibody. The labeled precipitate was analyzed by SDS-PAGE. The positions of the DHBV-C, WHV-C, GSHV-C, and Δ157L species are indicated at the right. Sizes are indicated in kilodaltons at the left. (B) Analysis of mixed extracts. Oocytes were injected with a single transcript. ^{35}S-labeled lysates were combined in the indicated pairings and subjected to sucrose gradient fractionation and immunoprecipitation as described for panel A. Sizes are indicated in kilodaltons at the left.
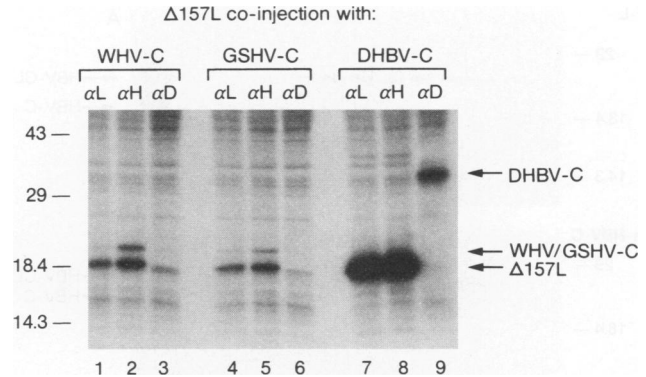
FIG. 4. Composition of dimer intermediates assembled in *Xenopus* oocytes coinjected with mRNAs encoding core proteins from different hepadnaviruses. Fractions 1 to 5 from the experiment of Fig. 3A, containing core dimer intermediates, were analyzed by immunoprecipitation exactly as described for the capsid fractions in the legend to Fig. 3. Designations are as for Fig. 3.

Analysis of coinjections of Δ157L with DHBV-C transcripts yielded very different results. Anti-L and anti-HBV-C, neither of which recognizes DHBV-C, immunoprecipitated only Δ157L (Fig. 3A, lanes 7 and 8); similarly, anti-DHBV-C antibody immunoprecipitated only DHBV-C (lane 9). This result shows that unlike the WHV and GSHV core proteins, DHBV-C and HBV-C cannot coassemble; when coexpressed, they yield separate homo-oligomeric capsid populations. This inability of mammalian and avian hepadnavirus cores to interact is not entirely unexpected given the significant divergence in their core protein sequences and their lack of immunologic cross-reactivity.

To rule out the formal possibility that the results supporting mixed capsid formation are due to nonspecific aggregations of different homocapsids immunoprecipitated by anti-L, we performed a mixing experiment control (Fig. 3B). Oocytes were injected with either HBV-C (Δ157L), WHV-C, or GSHV-C mRNA, so that only homo-oligomeric capsids can form. Pairs of lysates containing one tagged and one untagged C polypeptide species were then admixed and subjected to sucrose

gradient fractionation; capsid fractions were then immunoprecipitated as described earlier. In contrast to the coinjection experiments, under these conditions L antibody was able to immunoprecipitate very little WHV-C and GSHV-C (lanes 1 and 4) compared with anti-HBV-C immunoprecipitation (lanes 2 and 5). Not surprisingly, the mixing experiment involving DHBV capsids and HBV capsids likewise showed no interaction (lanes 7 to 9). These results indicate that only a small percentage of the signal indicating mixed capsid formation in the coinjection experiment is attributable to nonspecific interactions of homo-oligomeric capsids.

Hepadnavirus core dimerization is *cis* preferential. In authentic capsid assembly, dimers are the initial intermediates in assembly. We next set out to determine whether heterodimers form during mixed capsid assembly in oocytes. To do this, we examined gradient-purified dimer intermediates fractionated from the coinjected oocytes described above. Immunoprecipitation with anti-L revealed that Δ157L dimerized primarily with itself and formed few heterodimers with either WHV-C or GSHV-C (Fig. 4, lanes 1 and 4 versus lanes 2 and 5). There are two possible explanations for this result: (i) monomer-monomer affinity differences arising from sequence divergence favor homodimer formation over heterodimer formation in *trans*, or (ii) the dimerization process operates preferentially in *cis*; i.e., it favors the association of monomers translated from the same mRNA.

To distinguish between these two possibilities, we coinjected oocytes with SP6 transcripts encoding HBV-C and HBV-CL; here, the two proteins are identical except for the presence of the L epitope tag. Both proteins assemble into capsids with comparable efficiencies (data not shown). Coinjected lysates were fractionated on 3 to 25% sucrose gradients into 14 fractions. Each fraction was then immunoprecipitated with anti-L or anti-HBV-C and analyzed by SDS-PAGE. Under these sedimentation conditions, dimer intermediates sediment in fractions 3 to 10 and capsids pellet in fraction 14 (20). Coprecipitation of both chains with anti-L in fraction 14 confirms that mixed capsids form as expected (Fig. 5A). But precipitation of the dimer fractions with anti-L (Fig. 5A, lanes 3 to 10) clearly demonstrated that HBV-CL forms dimers primarily with itself rather than with HBV-C, despite the presence of HBV-C in these fractions, as revealed by precipitation with anti-HBV-C (Fig. 5B). Thus, the mixed capsids
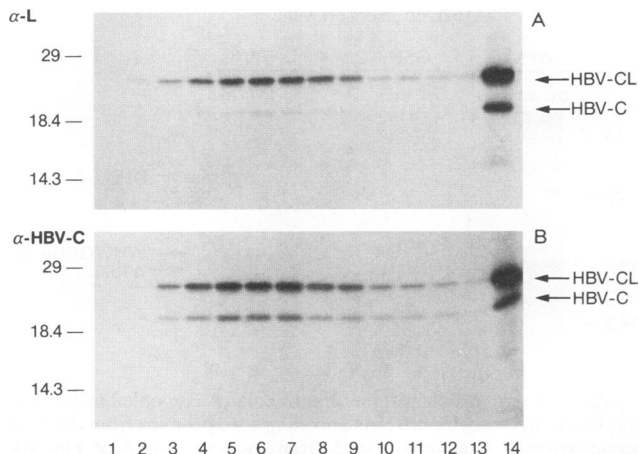
FIG. 5. Composition of dimer intermediates formed in *Xenopus* oocytes coexpressing tagged and untagged HBV-C. Oocytes were coinjected with mRNAs encoding HBV-C and the L-epitope tagged HBV-CL. ^{35}S-labeled lysates were resolved on 3 to 25% sucrose step gradients. Each of the 14 fractions was immunoprecipitated under nondenaturing conditions with either an anti-L MAb (α-L; A) anti-HBV-C polyclonal antibody (α-HBV-C; B) and analyzed by SDS-PAGE. Note that dimer intermediates sediment in fractions 3 to 10, and capsids pellet at the bottom (fraction 14). Sizes are indicated in kilodaltons at the left.

assembled in the coinjected oocytes (Fig. 5, lanes 14) must be composed predominantly of homodimers of tagged and untagged C chains.

Using a PhosphorImager to quantitate the amount of HBV-C and HBV-CL produced, we estimate that approximately 35% of dimers found in the coinjection experiment should have been heterodimers, assuming free and random association of HBV-C and HBV-CL monomers leading to a binomial distribution of dimer products. In fact, if we correct for antibody cross-reactivity and immunoprecipitation efficiencies, our results show that heterodimers account for at most 7% (and probably less) of the dimer pool. These findings indicate that C proteins display a marked *cis* preference for dimerization in the oocyte. Possible explanations for this will be considered below.

DISCUSSION

Sequence requirements for core-core interactions. We have used the two-hybrid system in a permissive human hepatoma cell line (HepG2) to characterize core protein interactions involved in HBV capsid assembly. We have shown that the full-length core protein fused downstream of the GAL4 or VP16 domain is able to associate with itself; this association, which normally occurs in the cytoplasm, must have stably persisted in the nucleus, where the host RNA polymerase II is located.

Core fusions with a truncation of the C-terminal 41 aa also oligomerized with full-length cores, as predicted from in vivo capsid assembly experiments. A deletion that extended 68 aa upstream from the C terminus failed to interact; this result also agrees with findings from earlier assembly studies (2, 3). The effect of N-terminal deletions on core-core association has not been previously reported. We engineered core fusions lacking the first 28 and 37 residues from core; neither deletion construct oligomerized with the full-length core fusion. Unfortunately, one of the major limitations in using the two-hybrid

assay is that only fusions that yield a positive CAT signal are informative. Fusions that fail to associate with core in this assay may indeed lack a domain critical for core interaction, or they may have simply folded into an improper conformation or be unstable. The fact that the full-length and the Arg tail-deficient core fusions were able to associate suggests that the GAL4 and VP16 domains are discrete structures that did not interfere with the folding of the C portion of the fusion. We favor the view that the assembly-defective deletions may have globally disrupted the secondary and tertiary structure of the core polypeptide. Although the core polypeptide structure has not been elucidated by crystallography, Agros and Fuller have proposed a structure based on modeling with the vp3 capsid protein of a picornavirus (1). Their sequence alignment analysis suggests that the core protein will adopt an eight-stranded antiparallel β-barrel structure, with most of the Arg-rich tail located distally. Both of the N-terminal deletions and the 68-aa C-terminal deletion would be predicted to remove at least two of the β strands and probably disrupt the secondary and tertiary structure important for intersubunit association. The structure of C protein may preclude the identification of a discrete contiguous domain that mediates core association; discontinuous residues critical to forming a contact surface during dimerization may be brought together only during the proper folding of the chain.

Assembly of mixed capsids in the *Xenopus* oocyte. Coexpression of Δ157L, a truncated and tagged HBV-C, with WHV-C or GSHV-C led to the assembly of mixed capsid particles. Coexpression of Δ157L and DHBV-C, which differs considerably in sequence and size from the mammalian cores, did not lead to the formation of mixed capsids. Assembly of HBV-C into capsids in the oocyte proceeds without detectable assembly intermediates other than dimers (20, 21); our coexpression experiments with the animal viral cores also failed to reveal any higher-molecular-weight assembly intermediates in hetero-oligomeric capsid formation. A number of explanations for this are possible. Most likely, such intermediates are extremely transient as a result of the efficient and highly cooperative assembly of capsids from dimer building blocks (15, 20); alternatively, they may be unstable in cell extracts or may dissociate during centrifugation.

Our results with the oocyte assembly system raise the intriguing issue of whether mixed nucleocapsids can form during hepadnavirus replication. Such a situation could occur in vivo for WHV and GSHV, since both can replicate in woodchuck hosts (14a). Hybrid nucleocapsids might affect several processes in the hepadnavirus life cycle. Cores are intimately involved in RNA encapsidation, DNA synthesis, and viral budding. How a mixed nucleocapsid would affect the specificity or efficiency of any one of these process remains to be seen. There is little precedent for mixed nucleocapsid formation in other viruses with icosahedral capsids. In retroviruses, a recent report has demonstrated that mixed core particles between MuLV and HIV type 1 can be made, but only when artificial chimeric Gag precursors containing both HIV and MuLV determinants are coexpressed with wild-type MuLV Gag proteins (7). This finding suggests that homo-dimerization of the MuLV Gag proteins is the driving force for assembly, with the heterologous HIV sequences being incorporated as a result. As yet there have been no reports of mixed capsid formation between wild-type Gag proteins.

A *cis* preference in dimer formation. During the mixed capsid assembly reaction in *Xenopus* oocytes, the coexpressed core proteins formed primarily homodimers. Even when the coexpressed C polypeptides are identical except for the L epitope tag, homodimers still form preferentially. These results

indicate that core dimerization in the oocyte displays a strong *cis* preference. This suggests that core monomers are not free to diffuse and associate with other monomers and is consistent with the notion that dimerization occurs very rapidly after monomer production. In this view, a monomer is most likely to associate with the nearest monomer available in the region of its synthesis, i.e., those translated from the same polysome. In the extreme case, dimers may form cotranslationally between adjacent, nascent core polypeptides still tethered to the elongating ribosome. This may account for the absence of detectable monomers in the oocyte assembly system (20). Once formed, dimers are free to diffuse and associate with other dimers.

We do not know if this *cis* preference operates in mammalian cells, but this seems likely to be so. Our results in the mammalian two-hybrid system certainly do not exclude this possibility. Since GAL4 binds to DNA as a dimer (12), it is likely that the GAL4-core fusion proteins active in this assay are themselves dimeric and that all C-C interactions being detected in this system thus involve homodimers of C proteins.

ACKNOWLEDGMENTS

REFERENCES

1. **Argos, P., and S. D. Fuller.** 1988. A model for the hepatitis B virus core protein: prediction of antigenic sites and relationship to RNA virus capsid proteins. EMBO J. **7:**819–824.
2. **Beames, B., and R. Lanford.** 1993. Carboxy-terminal truncations of the HBV core protein affect capsid formation and the apparent size of encapsidated HBV RNA. Virology **194:**597–607.
3. **Birnbaum, F., and M. Nassal.** 1990. Hepatitis B virus nucleocapsid assembly: primary structure requirements in the core protein. J. Virol. **64:**3319–3330.
4. **Borisova, G., B. Arya, A. Dislers, O. Barschukova, V. Tsibinogin, D. Skrastina, M. Eldarov, P. Pumpens, K. Skryabin, and E. Grens.** 1991. Hybrid hepatitis B virus nucleocapsid bearing an immunodominant region from hepatitis B virus surface antigen. J. Virol. **67:**3696–3701.
5. **Clarke, B. E., S. E. Newton, A. R. Carrol, M. J. Francis, G. Appleyard, A. D. Syred, P. E. Highfield, D. J. Rowlands, and F. Brown.** 1987. Improved immunogenicity of a peptide epitope after fusion to hepatitis B core protein. Nature (London) **330:**381–384.
6. **Cohen, B., and J. Richmond.** 1982. Electron microscopy of hepatitis B core antigen synthesized in E. coli. Nature (London) **296:**677–678.
7. **Deminie, C. A., and M. Emerman.** 1993. Incorporation of human immunodeficiency virus type 1 Gag proteins into murine leukemia virus virions. J. Virol. **67:**6499–6506.
8. **Fearon, E. R., T. Finkel, M. L. Gillison, S. P. Kennedy, J. F.**

Casella, G. F. Tomaselli, J. S. Morrow, and C. V. Dang. 1992. Karyoplasmic interaction selection strategy: a general strategy to detect protein-protein interactions in mammalian cells. Proc. Natl. Acad. Sci. USA **89:**7958–7962.
9. **Fields, S., and O. Song.** 1989. A novel genetic system to detect protein-protein interactions. Nature (London) **340:**245–246.
10. **Hirsch, R., R. Colgrove, and D. Ganem.** 1988. Replication of duck hepatitis B virus in two differential human hepatoma cell lines after transfection with cloned viral DNA. Virology **167:**136–142.
11. **Luban, J., K. B. Alin, K. L. Bossolt, T. Humaran, and S. P. Goff.** 1992. Genetic assay for multimerization of retroviral Gag polyproteins. J. Virol. **66:**5157–5160.
12. **Marmorstein, R., M. Carey, M. Ptashne, and S. C. Harrison.** 1992. DNA recognition by GAL4: structure of a protein-DNA complex. Nature (London) **356:**408–414.
13. **Miyonahara, A., T. Imamura, M. Araki, K. Sugawara, N. Ohtomo, and K. Matsubara.** 1986. Expression of hepatitis B virus core antigen gene in *Saccharomyces cerevisiae*: synthesis of two polypeptides translated from different initiation codons. J. Virol. **59:**176–180.
14. **Nassal, M.** 1992. The arginine-rich domain of the hepatitis B virus core protein is required for pregenome encapsidation and productive viral positive-strand DNA synthesis but not for virus assembly. J. Virol. **66:**4107–4116.
14a. **Seeger, C., P. L. Marion, D. Ganem, and H. E. Varmus.** 1987. In vitro recombinants of ground squirrel and woodchuck hepatitis viral DNAs produce infectious virus in squirrels. J. Virol. **61:**3241–3247.
14b. **Seifer, M., and D. N. Standring.** 1993. Recombinant human hepatitis B virus reverse transcriptase is active in the absence of the nucleocapsid or the viral replication origin, DR1. J. Virol. **67:**4513–4520.
15. **Seifer, M., S. Zhou, and D. N. Standring.** 1993. A micromolar pool of antigenically distinct precursors is required to initiate cooperative assembly of hepatitis B virus capsids in *Xenopus* oocytes. J. Virol. **67:**4513–4520.
16. **Stahl, S. J., and K. Murray.** 1989. Immunogenicity of peptide fusions to hepatitis B virus core antigen. Proc. Natl. Acad. Sci. USA **86:**6283–6287.
17. **Standring, D. N.** 1991. The molecular biology of the hepatitis B virus core protein, p. 145–169. *In* A. McLachlan (ed.), Molecular biology of the hepatitis B virus. CRC, Boca Raton, Fla.
18. **Standring, D. N., J.-H. Ou, and W. J. Rutter.** 1986. Assembly of viral particles in Xenopus oocytes: pre-surface antigens regulate secretion of the hepatitis B viral surface envelope particle. Proc. Natl. Acad. Sci. USA **83:**9338–9342.
19. **Zhou, S., and D. N. Standring.** 1991. Production of hepatitis B virus nucleocapsidlike core particles in *Xenopus* oocytes: assembly occurs mainly in the cytoplasm and does not require the nucleus. J. Virol. **65:**5457–5464.
20. **Zhou, S., and D. N. Standring.** 1992. Hepatitis B virus capsid particles are assembled from core-protein dimer precursors. Proc. Natl. Acad. Sci. USA **89:**10046–10050.
21. **Zhou, S., S. Q. Yang, and D. N. Standring.** 1992. Characterization of hepatitis B virus capsid particle assembly in *Xenopus* oocytes. J. Virol. **66:**3086–3092.